SNUTP-99-049
hep-ph/9911480

A new anomalous trajectory in Regge theory

Nikolai I. Kochelev[a*], Dong-Pil Min[b†], Yongseok Oh[b‡], Vicente Vento[c§], Andrey V. Vinnikov[d**]

[a] *Bogoliubov Laboratory of Theoretical Physics, JINR, Dubna, Moscow region, 141980 Russia*

[b] *Department of Physics and Center for Theoretical Physics, Seoul National University, Seoul 151-742, Korea*

[c] *Departament de Física Teòrica and Institut de Física Corpuscular, Universitat de València-CSIC E-46100 Burjassot (Valencia), Spain*

[d] *Far Estern State University, Sukhanova 8, GSP, Vladivostok, 690660 Russia*

(February 1, 2008)

Abstract

We show that a new Regge trajectory with $\alpha_{f_1}(0) \approx 1$ and slope $\alpha'_{f_1}(0) \approx 0$ explains the features of hadron-hadron scattering and photoproduction of the ρ and ϕ mesons at large energy and momentum transfer. This trajectory with quantum numbers $P = C = +1$ and odd signature can be considered as a natural partner of the Pomeron which has even signature. The odd signature of the new exchange leads to contributions to the spin-dependent cross sections, which do not vanish at large energy. The links between the anomalous properties of this trajectory, the axial anomaly and the flavor singlet axial vector $f_1(1285)$ meson are discussed.

PACS number(s): 12.40.Nn, 13.60.Le, 13.75.Cs, 13.88.+e

Typeset using REVTEX

*e-mail address: kochelev@thsun1.jinr.ru

†e-mail address: dpmin@mulli.snu.ac.kr

‡e-mail address: yoh@mulli.snu.ac.kr

§e-mail address: vento@metha.ific.uv.es

**e-mail address: vinnikov@thsun1.jinr.ru

I. INTRODUCTION

The descriptions of the total cross sections for elastic hadron-hadron, photon-hadron, and lepton-hadron scattering at large energy have been important issues in the understanding of QCD. Only a limited type of hadron reactions, the so-called hard processes, could be understood within the perturbative QCD. Most of the available data, however, deals with processes where the momentum transfer between the quarks and the gluons is relatively small and therefore their understanding should be the subject of nonperturbative studies. The latter are performed by the use of effective theories based on QCD. Regge theory is a well-known nonperturbative approach to hadron reactions [1]. It is based on the assumption that at large energy multi-particle exchanges with definite quantum numbers can be expressed by one effective particle exchange with its propagator given by the so-called Regge trajectory $(s/s_0)^{\alpha(t)}$. It was shown that one can fix the shape of the usual Regge trajectory $\alpha(t) = \alpha(0) + \alpha' t$ from the analysis of the mass spectrum M_J of the hadronic states with spin J, where $J = \alpha(0) + \alpha' M_J^2$ lies on this trajectory. Most Regge trajectories have the same slope $\alpha' \approx 0.9$ GeV^{-2}, which can be related with the universal value of the string tension between quarks, as has been found in lattice QCD calculations. The intercepts of the usual secondary Regge trajectories are not very large: $\alpha(0) \leq 0.5$.

The Pomeron trajectory, which was introduced into particle physics more than forty years ago, has properties which are very different from those of the other trajectories: It has the intercept larger than one, $\alpha_P(0) \approx 1.08$, and a slope $\alpha'_P \approx 0.25$ GeV^{-2}. These peculiar properties of the Pomeron play an important role in particle reactions, e.g., the Pomeron-exchange not only gives the main contribution to the total hadronic cross sections but also determines the behavior of the elastic differential cross sections at large energy and small momentum transfer.

The origin of the Pomeron-exchange has not yet been understood from QCD, but general wisdom ascribes its existence to the the *conformal anomaly* of the theory. This anomaly leads to finite hadron masses due to the non-vanishing of the matrix elements $\langle h|G^a_{\mu\nu}G^a_{\mu\nu}|h\rangle$ and vacuum energy density. The Landshoff-Nachtmann model [2] directly relates the properties of the soft Pomeron with the non-zero value of gluon condensate $\langle 0|G^a_{\mu\nu}G^a_{\mu\nu}|0\rangle$ and the nonperturbative two-gluon exchange between hadrons.

In addition to the conformal anomaly, QCD has also a non-conserved flavor singlet axial vector current due to the *axial anomaly*. This anomaly has played a crucial role in understanding the pseudoscalar meson spectrum. However only recently it has been clarified its importance for understanding the DIS spin-dependent structure functions. A solution to the proton spin problem (for a review see, e.g., Ref. [3]) due to the non-vanishing of the matrix element $\langle p|G^a_{\mu\nu}\widetilde{G}^a_{\mu\nu}|p\rangle$ has been suggested, where $\widetilde{G}^a_{\mu\nu} = \epsilon_{\mu\nu\alpha\beta}G^a_{\alpha\beta}/2$ is the dual to the gluon tensor $G^a_{\mu\nu}$. Within supersymmetric QCD only some definite chiral combinations of these two tensors, $GG \pm iG\widetilde{G}$, correspond to superfields [4]. Therefore the matrix elements $\langle h|G^a_{\mu\nu}G^a_{\mu\nu}|h\rangle$ and $\langle h|G^a_{\mu\nu}\widetilde{G}^a_{\mu\nu}|h\rangle$ can be related to each other. This link was used in Ref. [4] to estimate the value of the flavor singlet axial vector charge of the proton. Does this relation hold also in real QCD?, and if so, what are its implications in Regge phenomenology? If this relation holds, it would be natural that, *in addition to* the Pomeron trajectory, a new anomalous Regge trajectory would exist, associated to the vacuum properties of QCD through the axial anomaly and therefore with its quantum numbers. Our aim here is to show through data analysis that this possibility is indeed realized.

We will estimate the contribution of this trajectory to the elastic proton-proton scattering cross section and show it to be very important. We also compute the contribution of this trajectory to the photoproduction of the ρ^0 and ϕ mesons. Moreover we show that due to the specific quantum numbers of the possible exchanges, polarized and unpolarized proton-proton scattering and photoproduction of vector mesons can be very useful for investigating the possible consequences of this new trajectory.

The remaining part of this paper is organized as follows. In Sec. II the connection of the properties of the f_1 meson with axial anomaly is discussed. The effect of the new trajectory in proton-proton elastic scattering is evaluated in Sec. III. Section IV is devoted to the contribution of the f_1-exchange to the cross sections in ρ^0 and ϕ meson photoproduction. In Sec. V the contribution of the new trajectory to the polarization observables in *pp* collision and vector-meson photoproduction is obtained and its nontrivial role in polarized particle reactions is discussed. We give a short summary and some conclusions in Sec. VI.

II. PROPERTIES OF THE f_1 MESON AND THE PROTON SPIN

The small value of the flavor singlet axial vector charge g_A^0 which was measured by EMC [5], led to the crisis of the naive parton model for the polarized deep-inelastic scattering [3]. Despite the understanding that the fundamental origin of this phenomenon is related to the non-conservation of the flavor singlet axial vector current due to axial anomaly, the explicit calculation for the value of the flavor singlet axial vector charge within QCD is absent so far [6]. The main problem here is the poorly known nonperturbative sector of QCD, which does not allow to perform exact calculations. One possible way to explain the small value of g_A^0 is to investigate its connection with the effects of the axial anomaly in meson spectroscopy, and there have been many trials to connect the polarized DIS anomaly with the anomalous properties of the η' meson, e.g. through the $\mathrm{U}(1)_A$ problem. However, it should be mentioned that because of its quantum numbers the pseudoscalar η' meson cannot give a *direct* contribution to the double spin asymmetry in polarized DIS, which was used to extract the value of the forward flavor singlet *axial vector* current matrix element,

$$\langle p|\sum_q \bar{q}\gamma_5\gamma_\mu q|p\rangle = 2\, m_p g_A^0 S_\mu, \tag{1}$$

where m_p is the proton mass and S is its spin. It is evident that only flavor singlet axial vector mesons can contribute to the left hand side of this equation.

There are three axial vector mesons with the appropriate quantum numbers $[I^G(J^{PC}) = 0^+(1^{++})]$ contribute to this matrix element: $f_1(1285)$, $f_1(1420)$, and $f_1(1510)$ [7]. The anomalous value of the nucleon matrix element of the singlet axial vector current implies an anomalous mixing for these axial vector mesons, similar to what happens in the case of the pseudoscalars. This mixing implies a strong violation of the OZI rule and therefore a strong gluonic admixture [8]. From the point of view of the present investigation the mixing is not important, what really matters is the role played by the lightest meson in this channel, the $f_1(1285)$, in the whole procedure. This meson behaves in the vector axial three isosinglet case in the same way as the η' behaves in the pseudoscalar case, namely it saturates the anomaly. It is the purpose of this paper to estimate the effects of the $f_1(1285)$-exchange in elastic nucleon-nucleon scattering and vector-meson photoproduction, and in so doing display the special role played by its Regge trajectory, as a consequence of the properties of the vacuum of QCD. Throughout this paper, f_1 stands for the $f_1(1285)$ state and we will neglect the possible admixture of the other hadronic states to the wave function of the f_1-meson.

Let us briefly review some of the results of Sec. III of Ref. [8] to adapt them to our purpose. The matrix element of the axial vector current can be rewritten as a sum over all possible intermediate states by using the idea of the axial vector dominance:

$$\langle N|\bar{q}\gamma_5\gamma_\mu q|N\rangle = \sum_{\substack{\mathcal{A} \\ k^2\to 0}} \frac{\langle 0|\bar{q}\gamma_5\gamma_\mu q|\mathcal{A}\rangle\langle\mathcal{A}N|N\rangle}{M_{\mathcal{A}}^2 - k^2}, \tag{2}$$

where $\mathcal{A}$'s are the axial vector meson states characterized by their corresponding flavor quantum numbers. This expression provides relations between the axial charges of the nucleon and the coupling constants of the axial vector mesons with the nucleon,

$$\langle\mathcal{A}N|N\rangle = ig_{\mathcal{A}NN}\bar{u}(p')\gamma_\mu\gamma_5 u(p)\varepsilon^\mu, \tag{3}$$

given by

$$g_A^3 = \frac{\sqrt{3}f_{a_1}g_{a_1NN}}{M_{a_1}^2}, \qquad g_A^8 = \frac{\sqrt{3}f_{f_8}g_{f_8NN}}{M_{f_8}^2}, \qquad g_A^0 = \frac{\sqrt{3}f_{f_1}g_{f_1NN}}{M_{f_1}^2}. \tag{4}$$

Here the decay constants are defined by

$$i\varepsilon_\mu f_A = \langle 0|\bar{q}\gamma_\mu\gamma_5 q|(\bar{q}q)_A\rangle, \tag{5}$$

and ε_μ is the polarization vector of the meson. The eighth component of the flavor octet f_8 will be identified with the $f_1(1420)$ [7].

From the data on the decay of $\tau^- \to a_1^- + \nu_\tau$ one obtains [8]

$$f_{a_1} = (0.19 \pm 0.03)\ \text{GeV}^2. \tag{6}$$

Then the first equation in Eq. (4) gives

$$g_{a_1NN} = 6.7 \pm 1.0. \tag{7}$$

The analogue with the F and D reduced matrix elements for the axial vector currents allows to estimate the coupling constant of the flavor singlet axial vector meson with the nucleon as in Ref. [8]:

$$g_{f_1NN} = 2.5 \pm 0.5. \tag{8}$$

Note if we use the SU(3) relations for the decay constants of the axial vector meson octet, $f_{f_8} = f_{a_1}$, and the SU(6) relation between g_{f_1NN} and g_{f_8NN}, $g_{f_1NN} = \sqrt{2}g_{f_8NN}$, then we obtain a larger value, $g_{f_1NN} \approx 3.5$.

The last equation in Eq. (4) gives

$$f_{f_1} \approx 0.11 \text{ GeV}^2, \tag{9}$$

by using the axial vector charge

$$g_A^0 \approx 0.3, \tag{10}$$

which was found recently [10] by fitting the world data on the spin-dependent structure function $g_1(x, Q^2)$.

It should be mentioned that the estimates (9) and (10) are probably just *upper* limits for the corresponding magnitudes, because of the uncertainties in the extrapolation of flavor singlet part of the spin dependent structure function $g_1(x, Q^2)$ to the low x region. At any rate we find that the violation of the SU(6) symmetry for the decay constants of axial vector mesons is very large and $f_{a_1} \approx 2 f_{f_1}$. A similar effect was discussed by Veneziano and Shore [11] for the case of pseudoscalar mesons. They have shown that the small value of the decay constant of the flavor singlet η_0 meson and g_A^0 is ascribed not to the properties of this meson itself but to the general properties of the QCD vacuum, namely to the phenomena of topological charge screening in the vacuum,

$$g_A^0 = \frac{\sqrt{6\chi'(0)}}{f_\pi} g_A^8, \tag{11}$$

where $\chi'(k^2) = d\chi(k^2)/dk^2$ and $\chi(k^2)$ is the so-called topological susceptibility,

$$\chi(k^2) = i \int dx e^{ikx} \langle 0 | T \frac{\alpha_s}{8\pi} G\widetilde{G}(x) \frac{\alpha_s}{8\pi} G\widetilde{G}(0) | 0 \rangle. \tag{12}$$

Then the smallness of the decay constant f_{f1} can be thought to have the same origin, since using Eqs. (4) and (11) one can relate this constant with $\chi'(0)$,

$$f_{f_1} = \frac{\sqrt{3\chi'(0)}}{f_\pi} f_{f_8}, \tag{13}$$

where we have neglected the mass difference of the f_1 and f_8.

From all of the above discussion we conclude that the properties of the f_1 are very different from those of the other mesons that belong to the same SU(6) multiplet, e.g. the a_1 and $f_1(1420)$ mesons. Furthermore they imply a dominating behavior in the cross sections when the f_1 meson contributes and which leads in general to unexpected and thereby anomalous results. In order to establish these facts in a concrete manner we proceed to calculate the contribution of the f_1 meson for two processes, elastic pp scattering at large $|t|$ and elastic photoproduction of ρ and ϕ mesons. These calculations will indeed show that the exchange of the f_1 meson produces important contributions in these processes.

Before we conclude this Section we would like to compare the f_1 with the anomalous Pomeron, for the reason that have been mentioned in the introduction. Equation (11) follows from the consideration of the *axial anomaly* contribution to the non-conservation of the flavor singlet axial vector current,

$$\partial_\mu J^{\mu 5}(x) = 2i \sum_q m_q \, \bar{q}\gamma_5 q + 2N_f Q(x), \tag{14}$$

where N_f is the number of flavors and

$$Q(x) = \frac{\alpha_s}{8\pi} G^a_{\mu\nu} \widetilde{G}^a_{\mu\nu} \tag{15}$$

is the topological charge density. Due to its relation with the axial anomaly, the properties of the f_1-exchange are related with the distribution of the topological charge in QCD vacuum. It is well-known that nonperturbative fluctuations of gluon fields called instantons give rise to the nontrivial topological structure of the QCD vacuum (see a recent review in Ref. [9]). The average size of the instantons in this vacuum is much smaller than the confinement radius,

$$\rho_c / R_{\mathrm{conf}} \approx 1/3. \tag{16}$$

Therefore the f_1-exchange should contribute to the hadronic cross sections at higher values of the momentum transfer than the Pomeron-exchange whose t-dependence is determined approximately by the isoscalar electromagnetic form factor of the hadrons participating in the process [12]. For the f_1NN vertex, we shall use the flavor singlet axial vector form factor

$$F_{f_1 NN} = 1/(1 - t/m^2_{f_1})^2, \tag{17}$$

with $m_{f_1} = 1.285$ GeV. This is comparable to the estimate of the isosinglet axial form factor of Ref. [13], which gives $F_A^0 = 1/(1-t/1.27^2)^2$ using the Skyrme model. Recent experimental data [14] on the flavor octet axial form factor favor $F_A^8 = 1/(1-t/1.08^2)^2$.

This form factor decreases slower with increasing $|t|$ than the isoscalar electromagnetic form factor of the Pomeron-nucleon vertex [12]:

$$F_1(t) = \frac{4m_p^2 - 2.8t}{(4m_p^2 - t)(1 - t/0.71)^2}, \tag{18}$$

where $1/(1-t/0.71)^2$ is the usual dipole fit. Therefore the f_1 contribution will dominate over the Pomeron contribution at large $|t|$. In this paper we will show explicitly this behavior in elastic proton-proton scattering and vector-meson photoproduction.

III. ELASTIC HADRON-HADRON SCATTERING

One very interesting feature of the available data on hadron-hadron scattering at high energy is their universality [15]. This means that at low momentum transfer $-t < 1$ GeV^2 and large energy $\sqrt{s} > 20$ GeV all data are described rather well by the Pomeron-exchange. It was shown also that the shrinkage of the diffractive peak with increasing energy can be explained by the following Pomeron trajectory,

$$\alpha_P(t) = \alpha_P(0) + \alpha'_P t, \tag{19}$$

with the Pomeron intercept $\alpha_P(0) \approx 1.08$ and slope $\alpha'_P \approx 0.25$ GeV^{-2}.

At $-t > 3$ GeV^2 and large energy, however, the experimental data for the differential cross sections for elastic proton-proton and proton–anti-proton scattering show a very different behavior. The differential cross sections in this kinematical region do not show *any* energy dependence and are only functions of the momentum transfer t. (see Fig. 1) Several explanations for the large $|t|$ data have been suggested. The most popular one is the Donnachie-Landshoff Odderon-exchange model based on a perturbative three-gluon exchange mechanism between nucleon quarks [15,16]. In this model, however, the average momentum transfer in each quark-quark subprocess in the experimental range of t is rather small, $-\hat{t} \approx -t/9 \leq 1.5$ GeV, and therefore justification for its applicability is still unclear [12]. (See also Ref. [17].) The validity of the perturbative approach to QCD to explain nucleon-nucleon elastic scattering data is even less clear for the Sotiropoulos-Sterman model [18] where a six-gluon effective exchange mechanism between nucleons was considered.

The new trajectory, which we relate to the effective f_1-exchange and to the manifestation of axial anomaly in the strong interaction, gives a more natural explanation to this experimental data. In this Section, we calculate the contribution of the f_1-exchange to the differential cross section for proton-proton elastic scattering at large energy, $s \gg m_p^2$ and $s \gg -t$;

$$\frac{d\sigma}{dt} = \frac{|T_{f_1}|^2}{16\pi s^2}. \tag{20}$$

The Lagrangian of the f_1-meson interaction with the nucleon for a point-like vertex is

$$\mathcal{L} = g_{f_1NN}\bar{\psi}_N\gamma^\mu\gamma^5\psi_N f_\mu, \tag{21}$$

which allows the f_1-exchange to generate non-spin-flip amplitudes in nucleon-nucleon scattering. The matrix element in Eq. (20) at $s \gg |t| \gg m_p^2$ reads

$$|T_{f_1}|^2 = \frac{4[g_{f_1NN}F_{f_1NN}(t)]^4 s^2}{(t - m_{f_1}^2)^2}, \tag{22}$$

which leads to the differential cross section of the elastic nucleon-nucleon scattering as

$$\frac{d\sigma}{dt} = \frac{[g_{f_1NN}F_{f_1NN}(t)]^4}{4\pi(t - m_{f_1}^2)^2}. \tag{23}$$

We note that it does *not* depend on the energy s.

In Fig. 1, we present the contribution from the f_1-exchange to the differential cross section for proton-proton elastic scattering and compare with the experimental data at large energies, $\sqrt{s} = 27.4$ GeV, 52.8 GeV, and 62.1 GeV, and large momentum transfer $|t| > 3$ GeV^2 [19]. In this calculation we have used $g_{f_1NN} = 2.5$, which was fixed by Eq. (8) through the proton spin analysis. The result shows that the f_1-exchange explains the experimental data on elastic proton-proton scattering at large momentum transfer very well.

The Pomeron contribution to the elastic pp scattering differential cross section [12,20,21],

$$\frac{d\sigma^P}{dt} = \frac{[3\beta_0 F_1(t)]^4}{4\pi}\left(\frac{s}{s_0}\right)^{2[\alpha_P(t)-1]} \tag{24}$$

with $\beta_0 \approx 2$ GeV^{-1} and $s_0 = 4$ GeV^2 is small at large $|t|$ compared with the f_1-exchange and can be neglected in this kinematical region. Of course at large energy the meson-exchange should be reggeized due to the contributions from the mesons of higher spin, $J = 3, 5, \ldots$, which belong to the same trajectory. As discussed above, however, there is a difference in the characteristic scales for the Pomeron and the new trajectory. In the former, the scale is determined by the interactions between quarks at the distance related to the confinement radius, while in the latter it is related to the axial charge distribution (16). Therefore the two trajectories should have different slopes and

$$\alpha'_{f_1} \approx \left(\frac{\rho_c}{R_{\mathrm{conf}}}\right)^2 \alpha'_P \approx 0.028 \text{ GeV}^{-2}. \tag{25}$$

The flatness of the new trajectory leads to small contributions of the heavier mesons to the cross sections. For example, with the slope (25) the next meson from the new trajectory with $J = 3$ should have a mass $M_{J=3} \approx 9$ GeV as determined from the equation,

$$J = \alpha_{f_1}(0) + \alpha'_{f_1} M_J^2. \tag{26}$$

In order to obtain a reasonable estimate we can safely neglect the contributions from the heavier mesons and take the contribution of the new trajectory as a fixed pole with $\alpha_{f_1}(t) = 1$.

The quantum numbers of this new trajectory are determined by the quantum numbers of the f_1 meson: The signature is $\sigma = -1$ with the parities $P = C = +1$. Thus the new trajectory should have the same contribution to pp and $\bar{p}p$ collisions. This property is different from the charge odd Odderon-exchange. Furthermore, the strength of the interaction of the new exchange with some hadronic state is determined by the value of the flavor singlet axial vector charge of the hadron. This leads to the vanishing of the contributions of this trajectory to the total cross sections of the elastic reactions πN, KN, $\pi\pi$, etc, because the axial vector charge of pseudoscalar mesons is zero. One further consequence of the dominance of the new trajectory is that at large $|t|$ the elastic πp cross section, that is determined by the Pomeron-exchange, should have very different t and s dependence in comparison with the pp case. The experimental data [22] support this conclusion.

One of the features of this new trajectory is that it is responsible for the *spin dependence* of the lepton-hadron, photon-hadron, and hadron-hadron cross sections at large energies. Thus the exchange of this trajectory should determine the behavior of the flavor singlet part of the spin-dependent structure function $g_1^N(x)$ at $x \to 0$:

$$g_1^N(x) \propto \frac{1}{x^{\alpha_{f_1}(0)}}, \tag{27}$$

where $\alpha_{f_1}(0) \approx 1$. Similar behavior with

$$\alpha_{f_1}(0) = 0.9 \pm 0.2 \tag{28}$$

for the neutron structure function was found by E154 Collaboration [23]. The peculiarity of the neutron structure function $g_1^n(x)$ is the smallness of the valence quark contribution. Therefore the behavior of this function is determined by the flavor singlet contribution in the experimentally available range of x. For the proton target the valence quark contribution is very large and the behavior in x follows the a_1 trajectory contribution in this range of x. Thus the neutron target is more suitable to investigate the new trajectory in polarized DIS.

IV. VECTOR MESON PHOTOPRODUCTION

The recent HERA data for vector-meson photoproduction [24–26] are now the subject for discussion in the different approaches [27]. The interest to these data is related to the possible check of different nonperturbative and perturbative QCD models for particle photoproduction. In spite of the success of several models in the description of some properties of vector-meson photoproduction, a complete theory is not available so far. Indeed, the new ZEUS data for ρ, ϕ, and J/ψ photoproduction [26] show that the perturbative approach may describe only J/ψ photoproduction. We also note that the nonperturbative approaches based on the dominant contribution of the *universal* Pomeron trajectory fail to explain the cross sections at large momentum transfer $|t|$. Furthermore, the mechanisms which are responsible for the specific polarization properties of the electromagnetic production of vector mesons has not been clarified until now. For example, it is very hard for such models to explain the large double spin asymmetry in ρ meson electroproduction at relatively small value of Q^2 observed recently by the HERMES Collaboration [28].

The specific features of the new trajectory can be extracted from the experimental data of vector-meson production. As we discussed above, because of the different t-dependence of the form factors in the Pomeron-nucleon and f_1-nucleon vertices this new trajectory should dominate over the Pomeron contribution at large $|t|$ region. To demonstrate the effect of the new trajectory we present here the numerical results for ρ^0 and ϕ photoproduction at large energy W, where $W^2 = (p+q)^2$ is the center of mass energy of the photon-nucleon system. (Definitions of the kinematical variables can be found in Fig. 2.) We consider contributions from the two processes shown in Fig. 2. The contributions from π and η exchanges which give corrections to the diffractive process at low energy [29] are suppressed at large energy and are not considered in this work.

It is very well-known that the t-channel exchange by the Pomeron trajectory gives the main contribution to the cross sections of vector-meson photoproduction at small $|t|$. The matrix element of this exchange within the Donnachie-Landshoff model reads [12,21,29–31]

$$T_{\lambda_V,m';\lambda_\gamma,m} = i12\sqrt{4\pi\alpha_{\rm em}}\beta_u G_P(w^2,t)F_1(t)\frac{m_V^2\beta_f}{f_V}\frac{1}{m_V^2-t}\left(\frac{2\mu_0^2}{2\mu_0^2+m_V^2-t}\right)$$
$$\times\left\{\bar u_{m'}(p')\not q\, u_m(p)\varepsilon_V^*(\lambda_V)\cdot\varepsilon_\gamma(\lambda_\gamma) - \left[q\cdot\varepsilon_V^*(\lambda_V)\right]\bar u_{m'}(p')\gamma_\mu u_m(p)\varepsilon_\gamma^\mu(\lambda_\gamma)\right\}, \quad (29)$$

where the vector-meson and photon helicities are denoted by λ_V and λ_γ while m and m' are the spin projections of the initial and final nucleon, respectively,

$$G_P(w^2,t) = \left(\frac{w^2}{s_0}\right)^{\alpha_P(t)-1}\exp\left\{-\frac{i\pi}{2}[\alpha_P(t)-1]\right\}, \quad (30)$$

with $w^2 = (2W^2 + 2m_p^2 - m_V^2)/4$, and $F_1(t)$ is given in Eq. (18). The vector-meson mass is m_V and $\alpha_P(t)$ is the Pomeron trajectory given by Eq. (19) with $\alpha_P(0) = 1.08$ and $\alpha_P' = 1/s_0 = 0.25$ GeV^{-2}. Other parameters are

$$\mu_0^2 = 1.1\ \text{GeV}^2, \qquad \beta_u = \beta_d = 2.07\ \text{GeV}^{-1}, \qquad \beta_s = 1.45\ \text{GeV}^{-1}, \quad (31)$$

and the vector-meson decay constants are $f_\rho = 5.04$ and $f_\phi = 13.13$.

The vertex for the coupling of the axial vector current (with momentum q and polarization vector ξ^μ) with two vector currents (with momentum $k_{1,2}$ and polarization vectors $\epsilon^\mu_{1,2}$), i.e. $1^{++} \to 1^{--}1^{--}$, can be described by two form factors [32],

$$M_{f_1VV} = \varepsilon_1^\alpha \varepsilon_2^{\beta *} \xi^\mu \epsilon_{\alpha\beta\mu\delta} \left[A_2(k_1,k_2) k_1^2 k_2^\delta + A_2(k_2,k_1) k_2^2 k_1^\delta \right], \tag{32}$$

where $A_1(k_1,k_2) = -A_2(k_2,k_1)$. Note that in general there are six form factors and two of them do not contribute to the physical processes. Here we follow the prescription of Ref. [33]. Therefore, for vector-meson photoproduction by the exchange of axial vector current, the structure of the vertex becomes very simple in the local limit with constant $A_1(k_1,k_2)$:

$$V_{f_1V\gamma} = g_{f_1V\gamma} \epsilon_{\mu\nu\alpha\beta} \xi^\beta \varepsilon_1^\nu \varepsilon_2^\alpha k_2^2 k_1^\mu, \tag{33}$$

where $k_2^2 = m_V^2$. This corresponds to the AVV interaction Lagrangian of Ref. [34] obtained by using the hidden gauge approach.

The coupling constant $g_{f_1V\gamma}$ can be determined from the experimental data on $f_1(1285) \to \gamma V$ decay [7]: $\Gamma(f_1 \to \rho^0\gamma) \simeq 1.30$ MeV and $\Gamma(f_1 \to \phi\gamma) \simeq 1.90 \times 10^{-2}$ MeV. The vertex form of Eq. (33) gives

$$\Gamma(f_1 \to V\gamma) = \frac{1}{96\pi} \frac{m_V^2}{m_{f_1}^5} (m_{f_1}^2 + m_V^2)(m_{f_1}^2 - m_V^2)^3 g_{f_1V\gamma}^2, \tag{34}$$

which leads to

$$|g_{f_1\rho^0\gamma}| = 0.94 \text{ GeV}^{-2}, \qquad |g_{f_1\phi\gamma}| = 0.18 \text{ GeV}^{-2}. \tag{35}$$

Therefore the matrix element of the f_1 meson exchange to elastic vector-meson photoproduction reads

$$\begin{aligned} T_{\lambda_V,m';\lambda_\gamma,m} = {} & i g_{f_1V\gamma} g_{f_1NN} F_{f_1NN} F_{f_1V\gamma} \frac{m_V^2}{t - m_{f_1}^2} \epsilon_{\mu\nu\alpha\beta} q^\mu \varepsilon_V^{*\nu}(\lambda_V) \varepsilon_\gamma^\alpha(\lambda_\gamma) \\ & \times \left(g^{\beta\delta} - \frac{(p-p')^\beta (p-p')^\delta}{m_{f_1}^2} \right) \bar{u}_{m'}(p') \gamma_\delta \gamma_5 u_m(p). \end{aligned} \tag{36}$$

For the form factor of the $f_1V\gamma$ vertex, $F_{f_1V\gamma}$, we take

$$F_{f_1V\gamma} = \frac{\Lambda_V^2 - m_{f_1}^2}{\Lambda_V^2 - t}, \tag{37}$$

with $\Lambda_\rho = 1.5$ GeV and $\Lambda_\phi = 1.8$ GeV.

The results for the Pomeron- and f_1-exchange contributions to the total cross sections of ρ and ϕ meson photoproduction are presented in Figs. 3 and 4. One can find that the f_1-exchange contribution is nearly constant with the energy and its magnitude is at the level of a few percent, say $\leq 5\%$, of that of the Pomeron-exchange. Figures 5 and 6 show the differential cross sections of ρ and ϕ meson photoproduction at $W = 94$ GeV. These show that the contribution of the f_1-exchange is very large and dominates over the Pomeron contribution in the large $|t|$ region. Therefore, although the f_1 contribution is suppressed in the total cross section, its role can be found in the differential cross sections.

V. NEW TRAJECTORY AND POLARIZED CROSS SECTIONS

The generic structure of the new trajectory can also be found from the spin dependence of the related vertices, which is very different from that of the Pomeron-exchange. The main difference is that this exchange has unnatural parity, i.e., $P = (-1)^{J+1}$. One expectation is then that the contribution of this new trajectory may be separated by measuring spin observables, for example, the double spin asymmetries in hadron-hadron, lepton-hadron, and photon-hadron interactions, which vanish in the natural parity Pomeron-exchange.

The wide experimental program for investigating polarization effects in proton-proton scattering has been suggested for RHIC [36]. The main goal of this program is to extract information about polarized parton distribution functions of the nucleon and to check the important role of the axial anomaly in polarization physics. We would like to emphasize that the polarized proton-proton *elastic* scattering could be very useful to extract the information about axial anomaly effects related with the contribution of the new trajectory.

As an example, we consider the effects of the f_1-exchange in the double longitudinal spin asymmetry in the pp elastic scattering:

$$A_{LL} = \frac{d\sigma(\rightleftarrows) - d\sigma(\rightrightarrows)}{d\sigma(\rightleftarrows) + d\sigma(\rightrightarrows)}, \tag{38}$$

where $d\sigma$ denotes the differential cross section of the proton-proton scattering and arrows show the relative orientation of the proton spins. This asymmetry can be written through the helicity amplitudes [37],

$$\begin{aligned} &\Phi_1 =<++\,|\,++>, \qquad \Phi_2 =<++\,|\,-->, \qquad \Phi_3 =<+-\,|\,+->, \\ &\Phi_4 =<+-\,|\,-+>, \qquad \Phi_5 =<++\,|\,+->, \end{aligned} \tag{39}$$

as

$$A_{LL} = \frac{-|\Phi_1|^2 - |\Phi_2|^2 + |\Phi_3|^2 + |\Phi_4|^2}{|\Phi_1|^2 + |\Phi_2|^2 + |\Phi_3|^2 + |\Phi_4|^2 + 4|\Phi_5|^2}. \tag{40}$$

It is very well-known that at large energy $s \gg |t|$ one can neglect the contribution to the cross sections from the spin-flip amplitudes, Φ_2, Φ_4, and Φ_5. Furthermore, the Pomeron- and f_1-exchanges have different relations for the Φ_1 and Φ_3 amplitudes:

$$\Phi_1^P = \Phi_3^P, \qquad \Phi_1^{f_1} = -\Phi_3^{f_1}. \tag{41}$$

Therefore only the interference between the two exchanges can lead to non-vanishing A_{LL}

$$A_{LL} \approx -\frac{2\Phi_1^{f_1}\,\mathrm{Re}(\Phi_1^P)}{|\Phi_1^P|^2 + |\Phi_1^{f_1}|^2}, \tag{42}$$

where we have neglected the contribution from the imaginary part of the f_1-exchange to A_{LL} because of the very small deviation of the intercept of new trajectory from one. Without this interference the asymmetry is suppressed as t/s. The final result for the asymmetry can then be written simply as

$$A_{LL} = \frac{2\sqrt{d\sigma^P d\sigma^{f_1}}}{d\sigma^P + d\sigma^{f_1}} \sin\left\{\frac{\pi}{2}[\alpha_P(t) - 1]\right\}, \tag{43}$$

where $d\sigma^{P(f_1)}$ is the contribution from the Pomeron- and f_1-exchange, respectively, to the differential cross section. The result of the calculation for the two RHIC energies, $\sqrt{s} = 50$ GeV and 500 GeV is presented in Fig. 7. This shows the large asymmetry at $|t| \leq 4$ GeV^2 and the weak dependence on the energy, which is related to the high intercept of the new trajectory.

Another very useful quantity which is also sensitive to the new trajectory is the difference of the total cross sections of polarized initial states:

$$\Delta\sigma_L = \sigma(\rightleftarrows) - \sigma(\rightrightarrows). \tag{44}$$

This asymmetry can be written in the terms of the helicity amplitudes,

$$\Delta\sigma_L = \frac{1}{2\sqrt{s(s-4m^2)}} \mathrm{Im}\left[\Phi_1(0) - \Phi_3(0)\right], \tag{45}$$

using the optical theorem. It should be mentioned that only unnatural parity exchange can contribute to $\Delta\sigma_L$. Since the Pomeron-exchange has $\Phi_1 = \Phi_3$, it does not contribute to $\Delta\sigma_L$ although it dominates in the unpolarized total cross section. Thus at large energy only the new anomalous trajectory which has unnatural parity can contribute. Since the asymmetry $\Delta\sigma_L$ is proportional to the imaginary part of the new trajectory, it vanishes if the intercept of the f_1 trajectory is $\alpha_{f_1}(0) = 1$ exactly. Therefore the measurement of this asymmetry at large energy gives the opportunity to measure the deviation of $\alpha_{f_1}(0)$ from one:

$$\Delta\sigma_L = \frac{2g^2_{f_1NN}}{m^2_{f_1}} \sin\left\{\frac{\pi}{2}[\alpha_{f_1}(0) - 1]\right\}. \tag{46}$$

Recently the E581/704 Collaboration [38] has reported a measurement on $\Delta\sigma_L$ for proton-proton scattering at rather large momentum $p = 200$ GeV/c:

$$\Delta\sigma_L = -42 \pm 48 \pm 53\ \mu b. \tag{47}$$

From this result, with assumption that at this energy the contribution of other Regge trajectories with unnatural parity is small, we can estimate the intercept of the new trajectory as

$$\alpha_{f_1}(0) = 0.99 \pm 0.04, \tag{48}$$

which is in good agreement with Eq. (28), which was extracted from the analysis on the behavior of the structure function $g_1^n(x)$ in polarized deep-inelastic scattering at low x.

Another suitable field to look for the effects of this trajectory is the polarized vector-meson photoproduction. Given in Fig. 8(a) are the results of the double spin asymmetries in ρ and ϕ photoproduction for longitudinally polarized proton targets and polarized photon beams at $W = 100$ GeV. We define the beam-target double asymmetry as

$$A_{LL}^V(t) = \frac{d\sigma(\rightleftarrows) - d\sigma(\rightrightarrows)}{d\sigma(\rightleftarrows) + d\sigma(\rightrightarrows)}, \tag{49}$$

where the arrows denote relative orientations of the proton spin and photon helicity. In Fig. 8(b) we also give $\bar{A}_{LL}^V(t)$ defined as

$$\bar{A}_{LL}^V(t) = \frac{\tilde{\sigma}(\rightleftarrows) - \tilde{\sigma}(\rightrightarrows)}{\tilde{\sigma}(\rightleftarrows) + \tilde{\sigma}(\rightrightarrows)}, \tag{50}$$

where

$$\tilde{\sigma}(t) \equiv \int_{|t|_{\min}}^{|t|} dt' \frac{d\sigma}{dt'}. \tag{51}$$

One can find that the values of A_{LL}^V and $\bar{A}_{LL}^V$ are very different from those of the Pomeron-exchange model. The f_1-exchange contribution gives rise to nonvanishing values for A_{LL}^V at small $|t|$ region, while the Pomeron model predicts $A_{LL} \approx 0$ at this region. It should be mentioned that recently the first measurements of the double spin asymmetries for vector-meson electroproduction was reported by the HERMES Collaboration [28]. They found large asymmetry for ρ meson electroproduction with $|t| \leq 0.4$ GeV^2. The asymmetries of ϕ and J/ψ electroproduction could not be measured accurately and cannot give any definite conclusion to these asymmetries. Nevertheless, the data on the double spin asymmetry of ρ electroproduction could not be explained by the Pomeron-exchange model and we propose the f_1-exchange as a possible candidate which gives nonvanishing double spin asymmetries at high energy.

VI. SUMMARY AND CONCLUSIONS

We have shown that the $f_1(1285)$ meson plays a very special role in some hadronic processes in the large energy and large momentum transfer region due to its special relation to the axial anomaly through the matrix elements of the axial vector current. This behavior is reminiscent of another effective particle with a very dominant behavior in hadron physics in this region, the Pomeron, whose relation with the conformal anomaly seems to be the motivation behind this behavior. Therefore it seems natural to describe the properties of the lightest f_1 in terms of Regge theory by associating to this resonance an anomalous trajectory, the odd signature companion of the even signature Pomeron. Our analysis of proton-proton scattering and vector-meson photoproduction has confirmed our suspicions. The contribution of the f_1-exchange to the cross sections of these processes does not depend on the energy, a clear signature of its anomalous Regge behavior.

We have found that the f_1-meson exchange can explain the differential cross sections of proton-proton scattering at large energy and large momentum transfer. The difference in the spin structure of the vertices of the f_1-trajectory from the Pomeron-exchange leads to their different contributions to the polarized proton-proton scattering and polarized vector-meson photoproduction. As a result, this trajectory gives non-zero values for the beam-target double spin asymmetries in both processes, and can be distinguished from the Pomeron-exchange model. These examples show the importance of the new trajectory in hadron reactions, and can be tested, for example, by the *pp2pp* experiment at RHIC [39], where a wide program to measure various spin-dependent elastic and total cross sections has been suggested. (See recent discussions in Ref. [40].)

As another test of the new trajectory, we suggest to investigate $b_1(1235)$ photoproduction, which decays mostly into $\omega\pi$. Since the b_1 has quantum numbers $I^G(J^{PC}) = 1^+(1^{+-})$, the empirical Gribov-Morrison rule [41] prohibits the Pomeron-exchange in this process, and because of the C parity vector-meson-exchanges such as ω and ρ cannot contribute. The possible pseudoscalar-meson exchange contribution, however, gives usually decreasing total cross section with the initial energy, while experiments [42] show approximately constant total cross section at large energies. Therefore, we expect that the new trajectory related with the f_1 may give important contribution to b_1 photoproduction. But the currently available data on this reaction [42] are very limited and new experiments at current electron facilities are strongly called for.

We also suggest to analyze the asymmetry P_σ of the two-meson decays of vector-mesons produced by linearly polarized photon beams [43]. Since this asymmetry is $+1$ for natural parity exchange and -1 for unnatural parity exchange, the f_1 contribution would be found from deviations of this quantity from $+1$ at large energy.

In summary, in the energy region of the analyzed experiments two trajectories, the Pomeron and the f_1, dominate the total cross sections and the asymmetries. And, therefore, this new anomalous Regge trajectory, which is responsible for spin effects at large energy, should be considered as a natural odd signature companion to the Pomeron.

ACKNOWLEDGMENTS

We are grateful to A. E. Dorokhov, S. B. Gerasimov, E. A. Kuraev, E. Leader, and T. L. Trueman for illuminating discussions. Y.O. is grateful to M. Tytgat for useful informations. D.-P.M. and Y.O. were supported in part by the KOSEF through the CTP of Seoul National University. V.V. was supported by DGICYT-PB97-1227, ERB FMRX-CT96-008, and the Theory Division at CERN, where part of this work was done.

REFERENCES

[1] P. D. B. Collins, *An Introduction to Regge Theory and High Energy Physics* (Cambridge Univ. Press, Cambridge, 1977).
[2] P. V. Landshoff and O. Nachtmann, Z. Phys. C **35**, 405 (1987).
[3] M. Anselmino, A. Efremov, and E. Leader, Phys. Rep. **261**, 1 (1995).
[4] J. H. Kühn and V. I. Zakharov, Phys. Lett. B **252**, 615 (1990).
[5] EM Collaboration, J. Ashman *et al.*, Phys. Lett. B **206**, 364 (1988), Nucl. Phys. **B328**, 1 (1989).
[6] H.-J. Lee, D.-P. Min, B.-Y. Park, M. Rho, and V. Vento, Nucl. Phys. **A657**, 75 (1999).
[7] Particle Data Group, C. Caso *et al.*, Eur. Phys. J. C **3**, 1 (1998).
[8] M. Birkel and H. Fritzsch, Phys. Rev. D **53**, 6195 (1996).
[9] T. Schäfer and E. V. Shuryak, Rev. Mod. Phys. **70**, 323 (1998).
[10] G. Altarelli, R. D. Ball, S. Forte, and G. Ridolfi, Acta Phys. Pol. B **29**, 1145 (1998); B. Lampe and E. Reya, Max Planck Inst. Report No. MPI-PHT-98-23, hep-ph/9810270; E. Leader, A. V. Sidorov, and D. B. Stamenov, Phys. Rev. D **58**, 114028 (1998), Phys. Lett. B **445**, 232 (1998); S. Scopetta, V. Vento, and M. Traini, Phys. Lett. B **421**, 64 (1998), Phys. Lett. B **442**, 28 (1998); P. Faccioli, M. Traini, and V. Vento, Nucl. Phys. **A656**, 400 (1999).
[11] G. M. Shore and G. Veneziano, Phys. Lett. B **244**, 75 (1990).
[12] A. Donnachie and P. V. Landshoff, Nucl. Phys. **B267**, 690 (1986).
[13] V. Bernard, N. Kaiser, and U.-G. Meißner, Phys. Lett. B **237**, 545 (1990).
[14] A. Liesenfeld *et al.*, Phys. Lett. B **468**, 19 (1999).
[15] A. Donnachie and P. V. Landshoff, Z. Phys. C **2**, 55 (1979), (E) **2**, 372 (1979); Phys. Lett. **123B**, 345 (1983); Nucl. Phys. **B231**, 189 (1984).
[16] B. Nicolescu, Talk at 8th EDS Blois Workshop, (1999) hep-ph/9911334.
[17] P. D. B. Collins and F. D. Gault, Phys. Lett. **112B**, 255 (1982).
[18] M. G. Sotiropoulos and G. Sterman, Nucl. Phys. **B419**, 59 (1994), Nucl. Phys. **B425**, 489 (1994).
[19] S. Conetti *et al.*, Phys. Rev. Lett. **41**, 924 (1978).
[20] P. V. Landshoff, Nucl. Phys. **B** (Proc. Suppl.) **18C**, 211 (1991).
[21] J.-M. Laget and R. Mendez-Galain, Nucl. Phys. **A581**, 397 (1995).
[22] R. Rubinstein *et al.*, Phys. Rev. D **30**, 1413 (1984).
[23] E154 Collaboration, K. Abe *et al.*, Phys. Rev. Lett. **79**, 26 (1997).
[24] ZEUS Collaboration, M. Derrick *et al.*, Z. Phys. C **63**, 391 (1994); Z. Phys. C **69**, 39 (1995); Phys. Lett. B **377**, 259 (1996); ZEUS Collaboration, J. Breitweg *et al.*, Eur. Phys. J. C **1**, 109 (1998); H1 Collaboration, S. Aid *et al.*, Nucl. Phys. **B463**, 3 (1996).
[25] J. A. Crittenden, Univ. Bonn Report No. BONN-HE-99-04, Talk at Workshop on Physics with Electron Polarized Ion Collider - EPIC '99, Bloomington, USA, Apr. 1999, hep-ex/9908023.
[26] ZEUS Collaboration, J. Breitweg *et al.*, DESY Report No. DESY-99-160 (1999), hep-ex/9910038.
[27] A. Donnachie and P. V. Landshoff, Nucl. Phys. **B311**, 509 (1989); A. Schäfer, L. Mankiewicz, and O. Nachtmann, Phys. Lett. B **272**, 419 (1991); J. R. Cudell, Nucl. Phys. **B336**, 1 (1990); M. G. Ryskin, Z. Phys. C **57**, 89 (1993); S. J. Brodsky *et al.*,

Phys. Rev. D **50**, 3134 (1994); T. Arens, O. Nachtmann, M. Diehl, and P. V. Landshoff, Z. Phys. C **74**, 651 (1997); D. Yu. Ivanov and R. Kirschner, Phys. Rev. D **58**, 114026 (1998); I. Royen and J.-R. Gudell, Nucl. Phys. **B545**, 505 (1999); L. L. Frankfurt, M. F. McDermott, and M. Strikman, JHEP **9902**, 002 (1999); S. V. Goloskokov, Eur. Phys. J. C **11**, 309 (1999); S. I. Manayenkov, DESY report No. DESY-99-016, hep-ph/9903405 (1999).

[28] HERMES Collaboration, A. Borissov, Talk at DIS-99, Zeuthen, Apr. 1999 (1999); HERMES Collaboration, F. Meißner, Talk at DIS-99, Zeuthen, Apr. 1999 (1999).

[29] A. I. Titov, Y. Oh, and S. N. Yang, Phys. Rev. Lett. **79**, 1634 (1997); A. I. Titov and Y. Oh, Phys. Lett. B **422**, 33 (1998); A. I. Titov, Y. Oh, S. N. Yang, and T. Morii, Phys. Rev. C **58**, 2429 (1998); Y. Oh, A. I. Titov, S. N. Yang, and T. Morii, Phys. Lett. B **462**, 23 (1999).

[30] A. Donnachie and P. V. Landshoff, Nucl. Phys. **B244**, 322 (1984).

[31] M. A. Pichowsky and T.-S. H. Lee, Phys. Rev. D **56**, 1644 (1997).

[32] L. Rosenberg, Phys. Rev. **129**, 2786 (1963).

[33] F. E. Close, Phys. Lett. B **419**, 387 (1998).

[34] N. Kaiser and U.-G. Meißner, Nucl. Phys. **A519**, 671 (1990).

[35] The Durham RAL Databases, http://durpdg.dur.ac.uk/HEPDATA/REAC.

[36] G. Bunce *et al.*, Physics World **3**, 1 (1992).

[37] G. L. Kane and A. Seidle, Rev. Mod. Phys. **48**, 309 (1976).

[38] E581/704 Collaboration, D. P. Grosnick *et al.*, Phys. Rev. D **55**, 1159 (1997).

[39] W. Guryn *et al.*, *pp*2*pp* Collaboration report for RHIC (1999).

[40] E. Leader and T. L. Trueman, Vrije Univ. Report (1999), hep-ph/9908221.

[41] V. N. Gribov, XIII International Conference on High Energy Physics, Berkeley, 1966 (unpublished); D. R. O. Morrison, Phys. Lett. **25B**, 238 (1967).

[42] Omega Photon Collaboration, M. Atkinson *et al.*, Nucl. Phys. **B243**, 1 (1984).

[43] K. Schilling, P. Seyboth, and G. Wolf, Nucl. Phys. **B15**, 397 (1970), (E) **B18**, 332 (1970); K. Schilling and G. Wolf, Nucl. Phys. **B61**, 381 (1973).

FIGURES

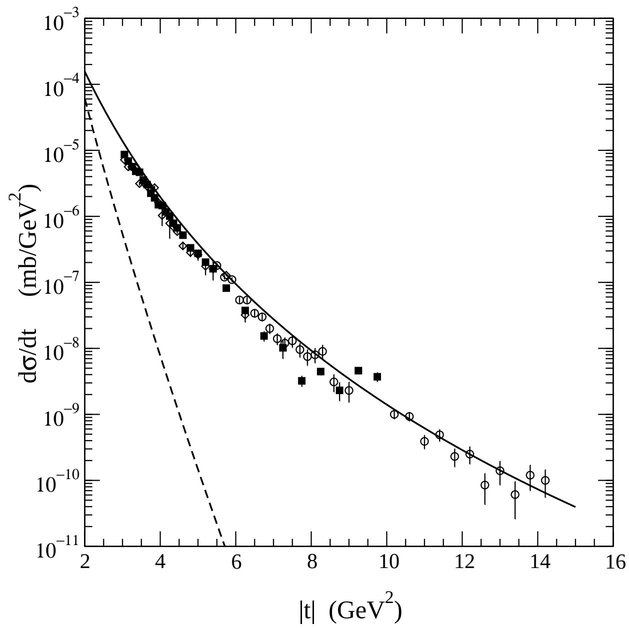

FIG. 1. The f_1-trajectory contribution to the differential cross section for the elastic proton-proton scattering at the large energy and momentum transfer. The solid line is the f_1 contribution while the dashed line is the Pomeron contribution at $\sqrt{s} = 27.4$ GeV. The data is from Ref. [19].

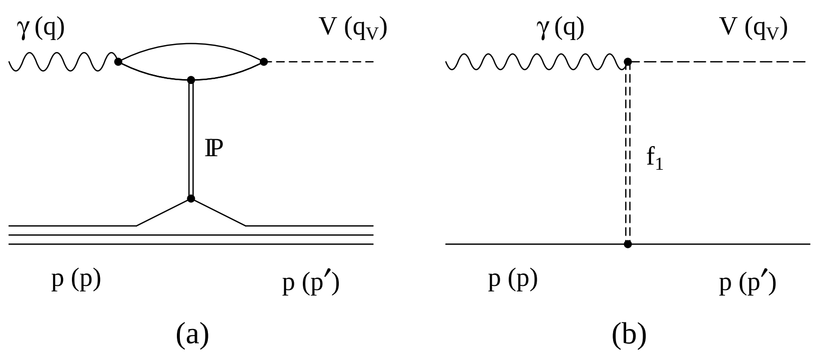

FIG. 2. Vector-meson photoproduction: (a) diffractive process by Pomeron-exchange and (b) f_1-exchange.

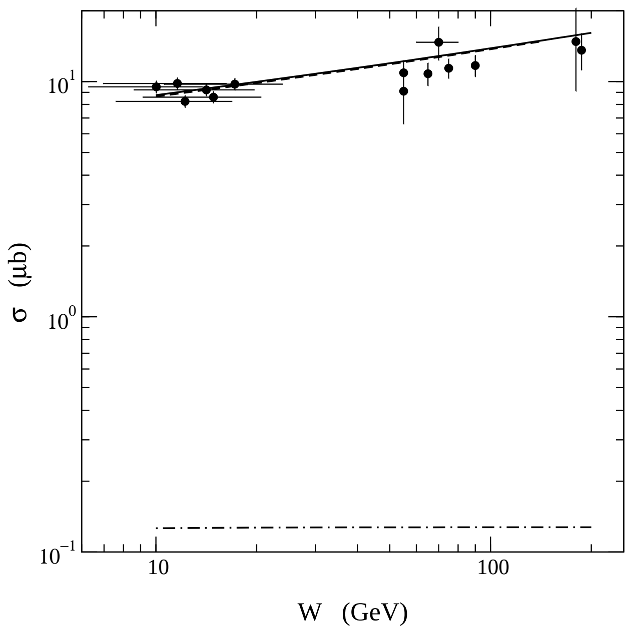

FIG. 3. The cross section for elastic ρ meson photoproduction. The dashed and dot-dashed lines are the contributions from the Pomeron- and f_1-exchange, respectively, while the solid line is the total cross section. The experimental data are from Refs. [24,35].

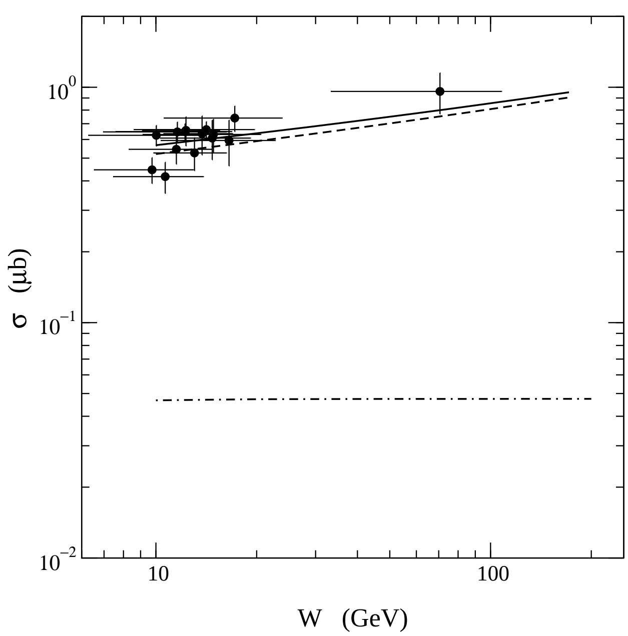

FIG. 4. The cross section for elastic ϕ meson photoproduction. Notations are the same as in Fig. 3.

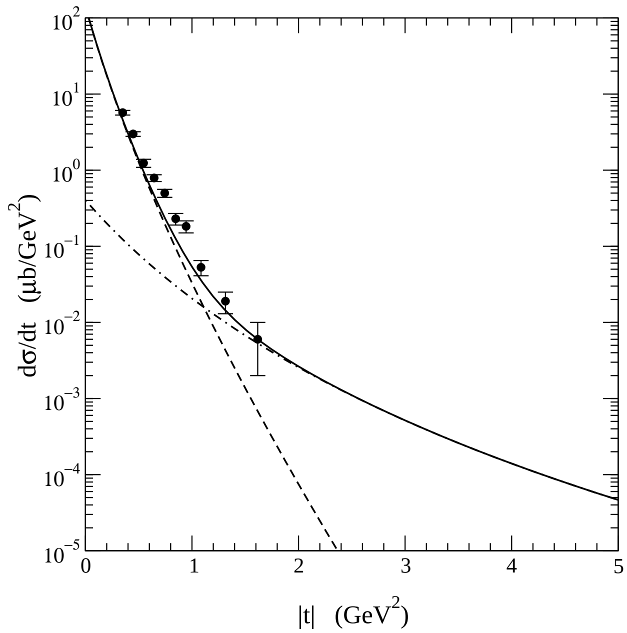

FIG. 5. The differential cross section for ρ meson photoproduction at $W = 94$ GeV. Notations are the same as in Fig. 3. Experimental data are from Ref. [26].

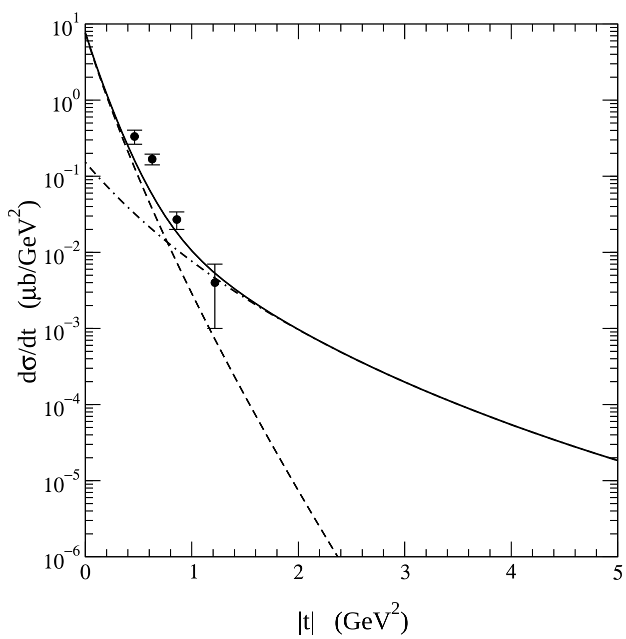

FIG. 6. The differential cross section for ϕ meson photoproduction at $W = 94$ GeV. Notations are the same as in Fig. 5.

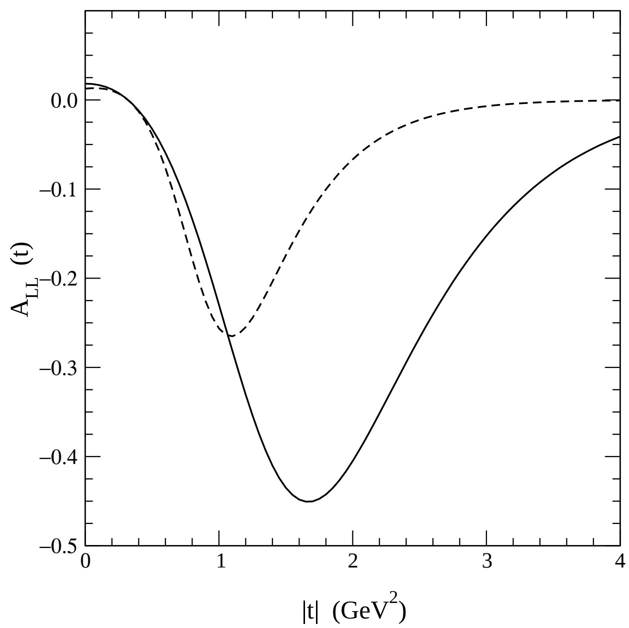

FIG. 7. The double longitudinal asymmetry in elastic proton-proton scattering at $\sqrt{s} = 50$ GeV (solid line) and at $\sqrt{s} = 500$ GeV (dashed line).

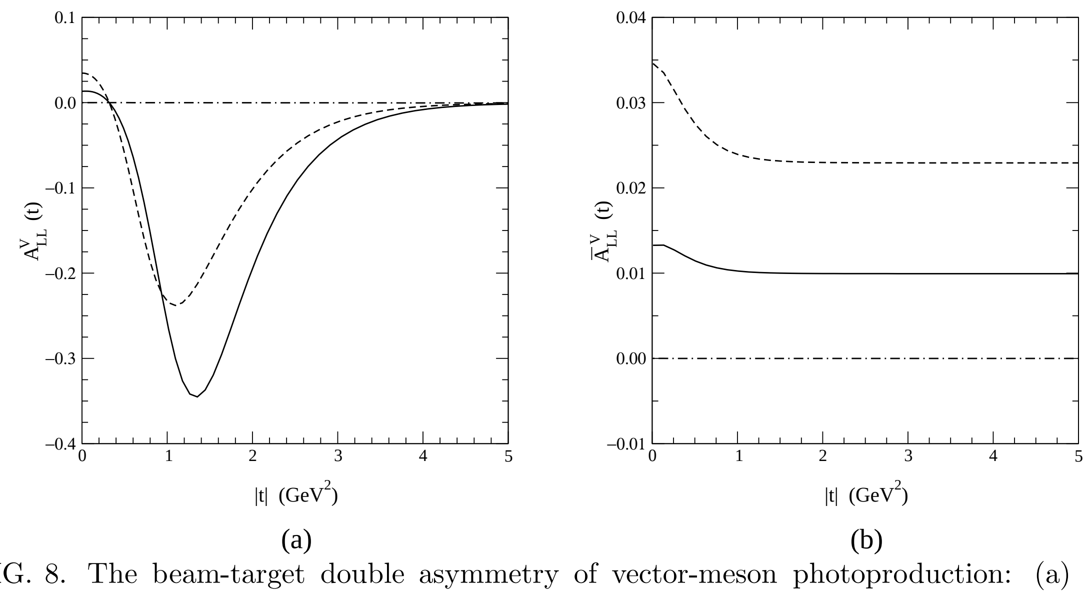

FIG. 8. The beam-target double asymmetry of vector-meson photoproduction: (a) $A^V_{LL}(t)$ and (b) $\bar{A}^V_{LL}(t)$ at $W = 100$ GeV. The solid and dashed lines correspond to the results with the f_1-exchange in ρ and ϕ production, respectively. The dot-dashed lines are the results of the Pomeron-exchange model for both cases.